REMARKS

Applicants have filed a Request for Continued Examination (RCE) herewith. Applicants have cancelled claims 1-21 and added new claims 22-46. Applicants believe that the claims presented in the present amendment patentably distinguish over the cited references. Applicants argue the patentability of the new claims with regard to the comments made by the Examiner and references cited by the Examiner in prior Office Actions.

Rejections under 35 U.S.C. 112, second paragraph

The Examiner has rejected previously entered claims, now cancelled, for reciting "a substrate" when "it appears from the specification and the drawings that the reference resistor and the flow-sensing resistor are formed on separate substrates..." Applicants have addressed Examiner's definiteness rejections by stating in independent claim 21: "a reference resistor element formed on a first electrically insulating substrate; a flow-sensing resistor element formed on a second electrically insulating substrate," and in independent claim 33: "a reference resistor element formed on a first segment of an electrically insulating substrate material...a flow-sensing resistor element formed on a second segment of said electrically insulating substrate material." Applicants further submit that independent claims 29 and 42 contain wording similar to claim 33 with regard to the resistor elements being formed on first and second segments of substrate material. Applicants submit that the claim wording in all of the newly entered claims conforms to the invention as described in the specification and the drawings. Thus, withdrawal of 35 U.S.C. 112, second paragraph rejections are requested.

Arguments in regards to Claims 22-41

The Examiner has cited Yamakawa et al. (U.S. Patent 6,314,960) as a primary reference in each of the three Office Actions: 9/14/01, 5/9/02, and 11/27/02. Applicants submit that Yamakawa et al. do not recognize that "said resistor elements are formed of an oxide electrically resistive material," which is a limitation in Applicants' independent claim 22. Furthermore, Applicants' independent claims 29 and 33 contain similar limitations. Within Yamakawa et al., the resistor material is described as "material such as platinum" in col. 3, line 39 and "formed of platinum or the like" in col.

3, line 52. Applicants submit that Applicants' "oxide electrically resistive material" is not "like platinum" or "such as platinum." Yamakawa et al. does not anticipate Applicants' "oxide electrically resistive material."

In the most recent office action of 11/27/02, the Examiner has combined the Yamakawa, et al. reference with Bischel (U.S. 6,444,297). Applicants submit that there is no motivation to combine Yamakawa et al. with Bischel. Yamakawa et al. teach a flow sensor with "heat generating resistors formed of heat-sensitive material such as platinum and deposited on the base film through vapor deposition, sputtering or the like process in the form of a thin film having a thickness of 0.2 μm" col. 8, lines 38-43. Bischel teaches a "method of producing a thick film metallization on an aluminum nitride substrate," per the title. The problem being solved by Bischel is in "providing an improved device reliability with regard to fastening pins or terminal assemblies onto the surface," col. 2, lines 8-10. There is no suggestion in Yamakawa, et al. of utilizing a thick film in place of the thin film. As will be discussed in the following, there is also no suggestion in Bischel that the thick film paste can be used as a heat generating or temperature sensing resistor. The Examiner states that: "Bischel teaches forming resistive heat-generating thick film elements from oxides." First, Applicants submit that the Examiner has misrepresented the Bischel reference. Nowhere in Bischel is there any reference to heat generation by the thick film circuit elements. In fact, Bischel teaches away from heat generation, as shown in the summary of the invention, column 2, lines 18-20: "The metallization layer forms a heat resistant firmly adhered metallic layer capable of being soldered or brazed" (emphasis added). However, even if Bischel showed a resistive heat-generating element, Bischel does not suggest or imply that the oxide layer can perform as an electrical resistor, because the buffering layer is an electrical insulator, as was the silicon nitride in Yamakawa et al. As is known to those skilled in the art, other than zero-resistance superconductors at cryogenic temperatures, all materials have some resistance to carrying electrical current. However, there is a distinction between being electrically resistive and performing as a resistor, particularly in place of the thin film Pt resistor of Yamakawa, et al. There is no recognition by Bischel that the thick film elements from oxide might be useful as a resistor element, let alone as a resistor element in a sensor application, which resistor, according to Applicants' invention, "has a temperature coefficient of resistance greater than 2500 ppm/°C." Applicants suggest that the Examiner uses hindsight when he

states: "One of ordinary skill in the art would have recognized the advantage and desirability of using oxides to form resistive elements in order to provide a thermally and mechanically stable structure." The combination shown in our invention is not obvious from the references cited by the Examiner.

As further evidence that combining the references is not obvious comes from the fact that metals have an extremely low value of the geometry-independent material property of resistivity which sets them apart from oxide materials in resistors. Because the resistivity of the thin film platinum-like resistors is significantly lower than the resistivity value of oxide resistors, the substitution is not obvious. Furthermore, the Yamakawa et al. resistors are formed in an expensive vacuum-chamber type process. The thick film oxide resistors are formed by economical screen printing and air-firing. The processes by which the two material types are formed are so distinct and cannot be substituted for each other, further leading one away from combining the references.

Applicants further submit that even if the combination proposed by the Examiner were proper, that the combination does not provide the claimed invention. In the 3rd Office Action, the Examiner states that Yamakawa, et al. shows Applicants' invention but "lacks a resistive material of an oxide used to form the resistors. Bischel teaches forming resistive heat-generating thick film elements from oxides." As discussed above, Applicants submit that the Examiner has misrepresented the Bischel reference because Bischel does not refer to any heat generation by the thick film circuit components. Bischel combined with Yamakawa et al does not show Applicants' claim 22 which contains the limitation: "with a temperature coefficient of resistance between 2500 and 4500 ppm/°C" referring to both resistor elements. If the thick film of Bischel were substituted for Yamakawa et al's thin film Pt material, Applicants' invention would not result. Because Yamakawa et al. do not provide information about the temperature coefficient of resistance suitable for the sensor's resistors, it would be impossible for Bischel to provide a resistor having "a temperature coefficient of resistance greater than 2500 ppm/°C," in the event that Bischel recognized that thick films could be used as resistors, which he does not.

In the 3rd Office Action, the Examiner has referenced Lee, et al. (U.S. 6,406,646). The Examiner states that "Lee teaches the use of Pb, Ru, Si, and Bi containing oxides for enhancing the adhesive strength of the film to the substrate." Applicants submit that Examiner's own words are evidence that there is no motivation to combine Lee et

al. with Yamakawa et al. Yamakawa et al. provide no motivation to look to Lee, et al. for "oxides for enhancing the adhesive strength of the film to the substrate." Yamakawa et al. teach: "resistors formed of heat-sensitive material such as platinum" col. 8, lines 38-39 to form a flow sensor. Nowhere does Yamakawa et al. discuss or recognize adhesion strength between the film and the substrate at all. There is no discussion in Lee, et al. concerning the oxides performing as resistors. Thus, there is no motivation for Yamakawa et al. to look to Lee, et al. or vice versa.

Even if the combination of Lee, et al. and Bischel with Yamakawa et al. were proper, it would not yield Applicants' claimed invention. The thick film oxides described in Lee, et al. (e.g., column 2, lines 26-28) have temperature coefficients of resistance of between -100 ppm/°C and +100 ppm/°C, as shown in G. M. Crosbie, F. Johnson, and W. Trela, "Processing Factor Dependence of Resistivity Parameters of Ruthenate-Based Thick Film Resistors With Low Temperature Coefficients," *J. Appl. Phys.* 84 [5] 2913-19 (1998), included as Attachment A. Thus, if the oxides described in Lee, et al. were substituted for the thin film Pt thin film material in Yamakawa et al., Applicants' invention, which shows "a temperature coefficient of resistance greater than 2500 ppm/°C," would not result.

Because there is no motivation to combine Yamakawa et al. with either Bischel or Lee, et al. and because a combination of Yamakawa et al. with either or both of Bischel and Lee et al. does not result in Applicant's invention, Applicants submit that newly added independent claims 22, 29, and 33 are allowable and such allowance is earnestly solicited. Furthermore, the Applicants request that dependent claims 23-28, 30-32, and 34-41, which depend from claims 22, 29, and 33, respectively, also be allowed.

<u>Arguments in regards to Claims 42-46</u>

Applicants' claim 42 contains the limitation: "printing a reference resistor element onto a first segment of an electrically insulating substrate and a flow-sensing resistor element onto a second segment of said electrically insulating substrate wherein said reference and flow-sensing resistor elements are comprised of a ruthenium-containing resistive oxide in a glassy matrix having a thickness between 2 and 30 μm."

In the 3rd office action of 11/27/02, the Examiner states: "Yamakawa as modified by Bischel does not explicitly disclose resistor thicknesses between 2 and 30

micrometers. Lee discloses a resistive thick film element of 10 micrometers (column 5, lines 55-65). One of ordinary skill in the art would have readily recognized the desirability and advantage of providing resistors having thicknesses between 2 and 30 micrometers in order to provide sensors that can quickly be heated to operating ranges of various electronic equipment."

Applicants submit that there is no motivation to combine Yamakawa et al. with Bischel or Lee et al., let alone combine all three references. As discussed above, neither the Bischel or Lee et al. references recognizes that thick film pastes can be used as resistors; in particular, the references are silent about thick film pastes being suitable for forming resistors in such a sensor application of Applicants, namely, a gas flow sensor. Yamakawa et al. do not mention or suggest replacing the thin film Pt, or Pt-like, resistor element with a thick film paste.

Because the combination of the references is improper, Applicants respectfully request allowance of independent claim 42 and claim 43-46 which depend therefrom.

Summary

Based on the foregoing comments, the above-identified application is believed to be in condition for allowance, and such allowance is courteously solicited. If any further amendment is necessary to advance prosecution and place this case in allowable condition, the Examiner is courteously requested to contact the undersigned by fax or telephone at the number listed below.

Please charge any cost incurred in the filing of this Amendment, along with any other costs, to Deposit Account No. 06-1510. If there are insufficient funds in this account, please charge the fees to Deposit Account No.06-1505.

Respectfully submitted,

Diana D. Brehob

Diana D. Brehob
Registration No. 51,496
Agent for Applicants

Date: 26-February-2003
Ford Global Technologies, Inc.
600 Parklane Towers East
Dearborn, Michigan 48126
(313) 322-1879
Fax: (313) 322-7162

Attachment A

Processing factor dependence of resistivity parameters of ruthenate-based thick film resistors with low temperature coefficients

Gary M. Crosbie,[a] F. Johnson,[b] and W. Trela
Ford Motor Company, 20000 Rotunda Drive, Dearborn, Michigan 48121-2053

(Received 16 February 1998; accepted for publication 26 May 1998)

Many analog sensor and control circuits take advantage of the low (<100 ppm/°C) temperature coefficient of resistance (TCR) of thick film resistors which are based on fired ruthenate-glass nanocomposites. To manufacture resistors with even smaller TCRs, a knowledge of the effects of processing on conduction mechanism parameters is of particular importance, because TCR is fixed in firing and cannot be trimmed later to a target value, as resistance can be. The peak firing temperature and time were varied, and a special four-probe dc design was used to minimize contact and printing nonuniformities. Corresponding to a greater energy level degeneracy in larger particles, the electrostatic charging energy decreased with the observed coarsening of the resistor microstructure. For the primary data set, the charging energy decreased (at >95% confidence) from 1.56 to 1.15 meV with increasing firing temperature (from 845 to 855 °C) and time (from 8 to 11 min). Model-based estimation of parameters is a means to provide quantitative understanding of how TCR and underlying conduction are controlled by process factors. © *1998 American Institute of Physics.* [S0021-8979(98)01517-5]

I. INTRODUCTION

Thick film resistors (TFR) are ceramic–glass composites with structures on a submicron scale which are used extensively in hybrid circuits for severe thermal cycling environments. Such resistors are desired because their electrical resistance can be formulated to be largely independent of temperature.[1] A better knowledge of how processing affects the remaining, small temperature dependence will allow improved calibration of analog conditioning circuits which must perform across a wide range of ambient temperatures, such as those required in automotive underhood sensors.

In the engineering community, the temperature coefficient of resistance (TCR)of TFRs is typically characterized by a pair of parameters [to be defined in Eq. (2)]: the hot- and cold-temperature coefficients of resistance (HTCR and CTCR), relative to 25 °C. Although these descriptors can serve as approximations (shown as secants in the example in Fig. 1) to the actual resistance versus temperature [$R(T)$] curve, they fit the data poorly and provide no insight into the conduction mechanisms. An increased understanding of how processing affects microstructure and model parameters dependent on that structure will allow better control of the process. In turn, this control would be beneficial to such products as a mass air flow sensor, which can have improved calibration from an analog signal conditioning circuit which exhibits minimal shifts in bridge resistance values in spite of large changes in temperature which are found in the automotive underhood environment.

Although thick film resistors have been extensively studied,[2–6] recent years have seen the advent of high resolution electron microscopy techniques that have reawakened interest in the physics and chemistry of these practical passive circuit elements. The goal in the present work is to give physical meaning to processing effects on microstructure and, in turn, resistance, through model parameters fitted to $R(T)$ curves. The approach taken is to modify a physically based model to allow fitting to compute the model's parameters for each specially designed and printed resistor measured for TCR. Factorial analysis[7] is then used to determine statistically the effects of processing factors on those parameters.

II. MICROSTRUCTURE DEVELOPMENT IN THICK FILM RESISTORS

TFR precursors are supplied as pastes comprised of small (≤10 nm) conductive metal oxide particles and larger (≈1 μm) glass frit particles dispersed in an organic vehicle.[1] After printing onto 96% Al_2O_3 substrates, the pastes are dried to remove the more volatile organic components. At this point the TFR microstructure can be described as a random array of glass spheres with conductive particles residing in the interstices and interfaces between the spheres. The TFRs are subsequently fired at a sufficiently high temperature (typically, around 850 °C) to allow liquid phase sintering of the glass to form a matrix phase. With lowered viscosity, the liquid (glass) wets the conductive particles and forms thin (1–2 nm) barrier layers between them. The resulting three-dimensional network of conductive particle chains leads to low magnetoresistance for use in low temperature TFR thermometers.[8] The glass barriers between the conductive particles are critical to the two-phase resistance model[2]

[a]Author to whom correspondence should be addressed (MD3182 SRL Bldg.); electronic mail: gcrosbie@ford.com
[b]Current address: Massachusetts Institute of Technology, Department of Materials Science and Engineering, Room 13-4154, 77 Massachusetts Ave., Cambridge, MA 02139.

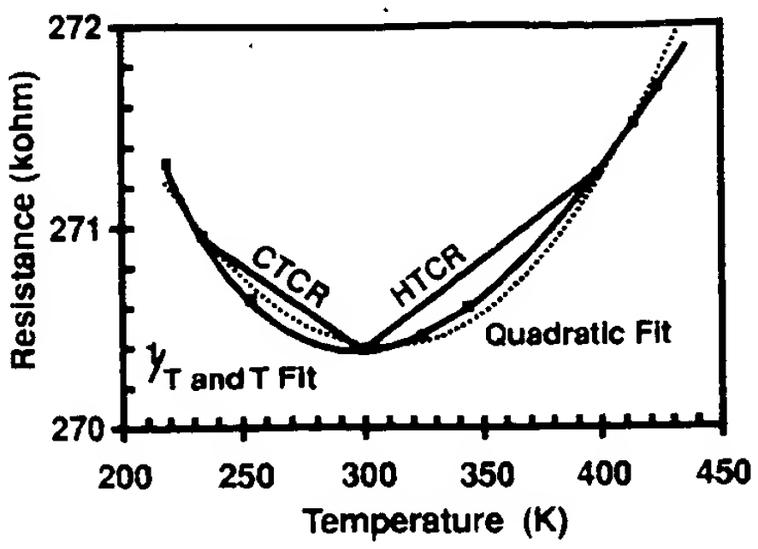

FIG. 1. Temperature dependence of resistance of a ruthenate thick film resistor fitted to different models: with engineering parameters for hot and cold TCRs illustrated as slopes of two secants; with a (T,T^2)-quadratic fit; and with the $(1/T,T)$ fit of the two-phase resistance model of Eq. (3). This example is from the "Production" set with peak firing at 845 °C for 8 min, where the greatest curvature of $R(T)$ is found. (*Courtesy of M. Hayes.*)

based on tunneling through those barriers that provides the excellent fit shown in Fig.1 near room temperature.

In characterizing TFR microstructures with transmission electron microscopy,[9] we earlier examined samples (corresponding to the secondary, "Lab" firing data set samples of the present work). Figure 2 is a representative structure from firing at peak temperature conditions of 10 min at 850 °C. Although there are a multitude of particles visible, only a fraction of them are conductive particles. In the system under study, the TFRs consist of two DuPont QS87 series resistor pastes blended to produce a nominal fired sheet resistivity of 56 kΩ/sq. The conductive particles were shown[9] by analytical electron microscopy (AEM) and x-ray diffraction (XRD) to be Pb–ruthenate ($Pb_2Ru_2O_{7-y}$) and CuBi–ruthenate ($Cu_xBi_{2-x}Ru_2O_{7-y}$). The remaining particles are Zr–silicate, which serve to adjust the thermal expansion coefficient of the ruthenate–glass composite to match more closely the ceramic substrate. Together with the issues due to the thin sampling section provided by the TEM foil and the low particle fraction needed for such a high resistance paste; it was found to be difficult to identify many conductive particle chains as distinguishable entities. The way to distinguish between the zircon and multiple ruthenate particle types was to collect an energy dispersive x-ray (EDX)spectru m for each particle. Longer firing times and higher peak firing temperatures were associated[9] with a coarsening of the conductive particles.

FIG. 2. Transmission electron micrograph of nanoscale structure of a thick film ruthenate resistor. This example is from the "Lab" firing set, with peak firing at 850 °C for 10 min, which is close to the center point of both "Production" and "Lab" data sets. (*Courtesy of W. T. Donlon.*)

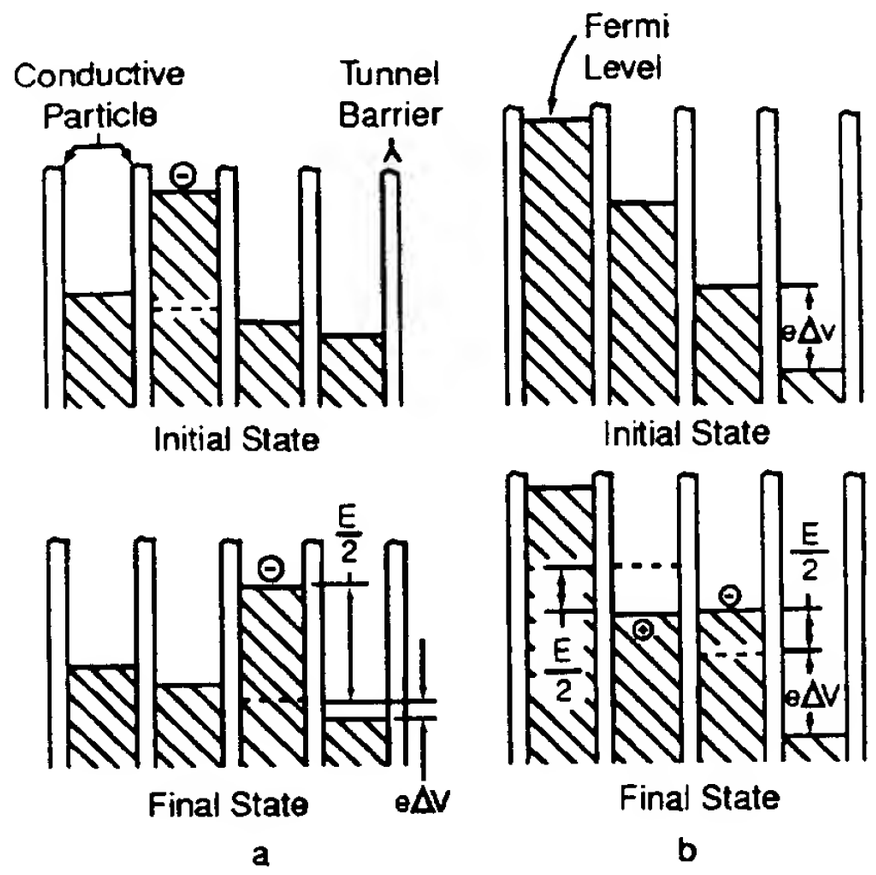

FIG. 3. Energy levels of two-phase resistance model. (a) Tunneling with thermally activated electrostatic charging in particles in negligible fields; (b) tunneling under an applied field (adapted from Ref. 11).

III. TWO-PHASE RESISTANCE MODEL

In a general thick film composite model based on a connected microstructure, the overall temperature dependence of resistance is determined by a summing of contributions of the conductive particles and the glass barriers between them. The conductive oxide particles exhibit a positive, essentially linear, increase with temperature that is characteristic of a metallic conduction. Of several glass barrier conduction models reviewed, Pike and Seager[2] conclude that the most likely is electron tunneling with impurities serving as resonant tunneling centers. Although planar, semi-infinite metal/interface/metal tunnel junctions have little temperature dependence near room temperature[10] a thermally activated character arises from the particulate geometry in TFRs. Since charge carriers within the ruthenate particles occupy discrete energy levels, a small, but nonnegligible, energy is required to alter the charge of the particles. This energy is referred to as an electrostatic charging energy by Pike and Seager[2] and others[11,12] and can be modeled by an Arrhenius term.

Figures 3(a) and 3(b) are diagrams[11] of the particle energy levels before and after tunneling, for (a) low field and for (b) high field cases, respectively. Under low applied fields that are typical of what would be encountered in an analog signal conditioning circuit, there would be a net drift of electrons towards the positive electrode and, conse-

quently, resistance would follow an ohmic behavior. Under high applied fields, field-induced tunneling would predominate and the V-I relationship would be highly nonohmic. Pike and Seager observed such high field results, which are consistent with resonant tunneling centers.[13–15]

It follows, then, that the $R(T)$ curve for a low field TFR is a sum of the resistance for the glass barriers and for the conductive particles. Pike and Seager [Eq. (8) of Ref. 2] give the following equation for the $R(T)$ curve:

$$R(T)=\frac{1}{2}R_{b0}\left[1+\frac{\sin(aT)}{aT}\right]\exp\left(\frac{E}{kT}\right)+R_{m0}(1+bT), \tag{1}$$

where T is the absolute temperature, a is related to the insulator barrier height, E is the electrostatic charging energy, k is Boltzmann's constant, b the ruthenate TCR, R_{b0} is the barrier preexponential factor, and R_{m0} is the metallic phase resistance if it were extrapolated to absolute zero.

The $\sin(aT)/aT$ term describes the weak temperature dependence of the tunneling itself.[10] Since the value of a is very low, around 10^{-4} K^{-1}, the $\sin(aT)$ term can be approximated by aT. The exponential term in Eq. (1) is used to estimate the equilibrium number of charged ruthenate particles in the system. The value of the activation energy has been measured[2,4] in other ruthenate systems to be of the order of 1 meV. The rightmost terms in Eq. (1) describe the temperature dependence of the resistance of the metallic ruthenate particles. The value of b is of the order of 500 ppm/°C.

Together, the terms of Eq. (1) form a rather flat $R(T)$ curve with a shallow minimum that can be placed near room temperature, as in the example of Fig. 1.

By way of contrast, industry convention characterizes the $R(T)$ curve with hot and cold TCR values. A typical equation[1] for calculating the secant TCRs is

$$\mathrm{TCR}=\frac{R(T_2)-R(T_1)}{(T_2-T_1)\times R(T_1)}\times 10^6. \tag{2}$$

Hot TCR is typically calculated between $T_1=25$ °C and a higher temperature, such as $T_2=125$ °C, and cold TCR is calculated between a lower temperature, such as $T_2=-40$ °C, and $T_1=25$ °C. In commercial TFRs, these secant TCRs can be within ±100 ppm/°C. As noted earlier, the Eq. (2) values only poorly approximate the curve (via the secant-chord slopes shown in Fig. 1) and do not provide insight into the conduction mechanism.

IV. EXPERIMENTAL PROCEDURE

A. Test pattern design and printing

Because of interest in the processing-induced changes to the materials chemistry and structure of the thick film resistor material, rather than pattern-size-dependent phenomena, steps were taken in the design of the test pattern and in the printing method to exclude contributions to the measurements from reactions with the terminations and from nonuniform cross-sectional areas.

The test pattern shown in Fig. 4 was designed for and used in all of the resistance tests reported in the present study. In this diagram, the printed ruthenate–glass resistor is the area that is filled in solid black. The rest of the pattern consists of the outlines of the underlying termination material, which is a Ag–Pd conductor–glass composite. Between the "current" pads are the two ordinary emf-sensing connections, which connect to the conductor, near the ends of the rectangular resistor pattern.

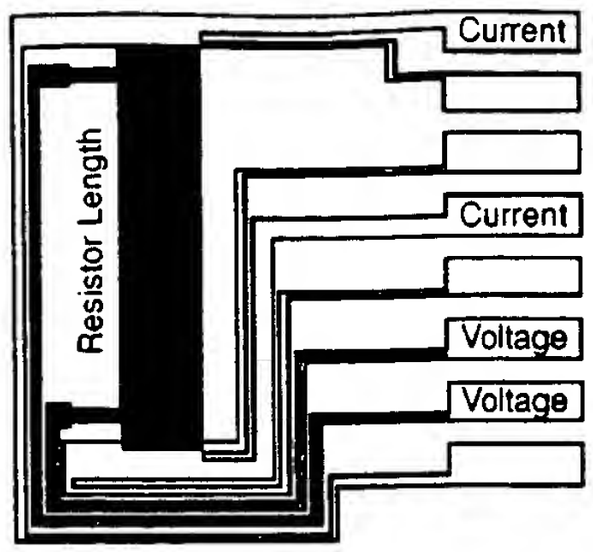

FIG. 4. The special four-probe dc specimen design. The ends of probes marked "voltage" are made of the resistor material itself at the points in contact with the section under test. Since these probes contact the test section away from any contact with the metallic terminations, the effects of any reaction with the metal contacts is excluded from the test section. (Additional electrodes, not named, allow other measurements which can include termination-related resistance contributions.)

Instead of using connections into the Ag–Pd terminations to measure emf, in the present work we used the alternate connections that are marked "voltage" in Fig. 4. The principal advantage is that any interdiffusion or reaction does not extend to the test section between these probes. (A reaction is known[5] to occur with Ag which lowers the viscosity of the resistor paste about 1 mm into a resistor as it is fired.) Since the "voltage" probes at their points of contact (defining the ends of the test section) are of the same material as the test section, compositional uniformity is maintained at those contacts. The design also provides advantages for low resistance paste tests: better parallelism of field lines in the test section because of the distance from the current terminations and exclusion of any series resistance at the fired resistor–conductor paste interface. The design gives a geometry of 4.375:1 for the width to the inner gauge length, to equal 4.375 sq.

The printing method was likewise chosen to minimize pattern-size-dependent interferences. In typical screen mesh printing, bowing of the screen causes the printed thickness (1) to be thinner at the center of a pattern than at the edges and (2) to be thicker adjacent to the (previously fired) conductor pattern, since the screen is lifted off the ceramic substrate there. In this work, the resistor layer was printed with an ink-dispensing system (Panasonic Byoga). This system provides "extrusion" of a constant volumetric flow of the paste. Coupled with a uniform transverse velocity of the nozzle, the cross-sectional area of the dispensed paste is kept uniform. The paste used was a blend of two DuPont QS87 series pastes (QS875 at 100 kΩ/sq, nominally, and QS874 at 10 kΩ/sq), which were mixed for a nominal sheet resistance of 56 kΩ/sq, but higher values were observed (average of cell averages of 91.1 kΩ/sq for the "Production" set), due mainly to a lower than nominal thickness.

TABLE I. Comparison of experimental conditions for the two firing studies which are identified as "Production" and "Lab" firings. Both are based on samples from the same printing set.

		Production	Lab
Furnace type		zoned belt	tube
Muffle material		Inconel	alumina
Firing zone width	(cm)	61	5
Peak temperature difference between High–Low levels	(°C)	10	50
Level=High	(°C)	855	875
Level=Low	(°C)	845	825
Temp. precision	(°C)	$\leqslant \pm 0.5$	$\approx \pm 10$
Time at peak temp difference between High–Low levels	(min)	3	4
Level=High	(min)	11	12
Level=Low	(min)	8	8
Time control		inverse of belt speed	manual insertion
Resistor count		52	12
Current applied during firing	(μA)	0	5 or 10
Delay between printing and firing firing	(day)	<1 day	≈750 day (dry box)

In the test pattern, the 4.8 mm width of the gauge section is produced by four passes of a 1.2 mm wide dispensing nozzle. The passes overlap slightly, causing thicker stripes to appear, but these arise parallel to the field lines. The cross-sectional uniformity that is obtained by such printing allows an experimental averaging (in each resistor image) over more resistor material than in typically sized TFRs.

After printing, samples were heated sufficiently to solidify the pastes by removing volatiles and then the test pieces were either fired immediately or stored under dry Ar. The as-dried resistor thickness was measured at 17 μm.

B. Firing equipment and data set identifiers

To form the resistor composites, the printed test samples were fired in two ways. The primary group, identified as "Production," is from firings that were run on a production thick film firing belt furnace (and is a subset of a larger process capability study). The secondary group, "Lab," is from firings carried out in a laboratory tube-furnace firing study,[9] which was originally intended only to be an exploration of *in situ* measurements of resistance during firing. In both sets, the resistor thickness after firing was about 8 μm, which is ~30% thinner than is typical. The two firing test conditions are compared in Table I. The sets are similar in that in both the peak firing temperature and time at peak temperature were the process factors which were varied in randomized two-level factorial designs.[7] However, the sets differed in the levels chosen for the factors, the precision of control of the temperature, the presence (or absence) of current flow during firing, the number of samples, and the delay time between printing and processing. Excellent control was achieved in matching target levels of the peak temperatures and times in the "Production" firing runs.

C. Curve fitting procedure

TCR measurements were made in a temperature controlled chamber (Model 4248B, Saunders Associates, Scottsdale, AZ). The boards were mounted in the chamber and the temperature was held, in sequence, at 25 °C, −40 °C, and 125 °C. After holding at target temperature for a minimum of 5 min, four-wire dc resistance measurements were made with a multiplexed Hewlett-Packard Model 3456 system voltmeter set for autoranging resistance.

Since three temperatures were used for most of the $R(T)$ data, some simplifications were required to fit these data to the two-phase resistance model. Specifically, the number of parameters to be fitted had to match the number of data points available (three) for each printed resistor image.

Since the $\sin(aT)/aT$ term is known to be close to unity in the five-parameter Eq. (1), we can exclude a from the fitting. In like manner, since the parameter E is expected to have a small value (relative to kT), on the order of 1000 μeV, the $\exp(E/kT)$ term can be approximated by $(1+E/kT)$. Pike and Seager[2] gathered extensive data on the temperature dependence of resistance of similar ruthenate particles which were extracted from a glass matrix by acid leaching. In all cases the parameter b, which estimates the ruthenate TCR alone, did not change. Therefore, it is reasonable to assume this parameter has a constant value[2] of 520 ppm/°C. These modifications lead from Eq. (1) to the following:

$$R(T)=R_{b0}\left(1+\frac{E}{kT}\right)+R_{m0}(1+bT), \tag{3}$$

where $b=520$ ppm/°C, T is in kelvin, and k is Boltzmann's constant. The result of these simplifications is a $(1/T,T)$ fit as shown as the solid curve in Fig. 1, which is shown in Fig. 1 to be an excellent fit to a "Production" firing set resistor which was measured at several intermediate temperatures. In this case, the regression produces a correlation coefficient, R^2, that is 0.99998 for this fit, but only 0.9860 for the (T,T^2) fit.

With only resistances for three temperatures, the parameters R_{b0}, E, and R_{m0} can be solved linearly from the $R(T)$ data for each resistor using Cramer's theorem, with basis values in the present work of 233, 298, and 398 K.

D. Unbalanced data set factorial analysis

At this point the data sets consist of the parameters fitted to resistance values for each resistor image. A standard effects analysis on the factors of peak firing time and time at peak temperature could not be performed directly because the data sets were unbalanced. That is, each combination of time and temperature did not have the same number of replicates. To avoid skewing the grand averages, a linear regression technique was identified that could appropriately adjust for the imbalances and give a statistical confidence for the main and interaction factor effects. The procedure is adapted

TABLE II. Effects analyses for "Production" and "Lab" firing data sets. For each model parameter, an average, three process factor effects, associated statistics, and normalizations are shown.

Parameter	Average	Effects					F_{obs}/F_{crit} Statistic		Normalized effects		
	(PD)	*A*:Temp (PD)	*B*:Time (PD)	*A*B* (PD)	Std. Err. (PD)	d.f.	R^2		*A*:Temp (PD×K^{-1})	*B*:Time (PD×min^{-1})	*C*: *A*B* (PD^2×K^{-1}×min^{-1})
Production firing 845–855 °C											
R_{b0} (Ω/sq)	60161	17486	9387	1377	295	48	0.9882	477.6	1748.6	693.0	2.51
E (eV×10^{-6})	1337	−214	−161	9	28	48	0.6390	10.1	−21.4	−17.1	0.56
R_{m0} (Ω/sq)	24098	1115	867	−228	186	48	0.5536	7.1	111.5	231.5	18.0
Lab firing 825–875 °C											
R_{b0} (Ω/sq)	62086	54649	39797	32786	3421	8	0.8202	3.0	1093.0	9949.0	163.9
E (eV×10^{-6})	1398	−371	−215	−291	139	8	0.3516	0.4	−7.4	−53.7	−1.46
R_{m0} (Ω/sq)	22321	11741	4496	510	1332	8	0.7420	1.9	234.8	1123.9	2.55

[a]PD denotes the model parameter dimension (units) of R_{b0}, E, and R_{m0}sh own in the leftmost column. For process span normalized effects, cell units are the PD divided by the high–low span units (e.g., "min" for the "*B*:Time" column).

from an example given by Vardeman.[16] In this linear model, the main and interaction effects are replaced by regression coefficients.

To perform the analysis, the variables x^{α} and x^{β} (from Vardeman[16]) were assigned a (contrast) value of −1/2 for each data point if the corresponding factor was at a low level (i.e., 8 min or 845 °C for the "Production" data set) or +1/2, if the factor was at a high level (i.e., 11 min or 855 °C for the same data set). A linear regression subroutine, "LINEST," supplied with Microsoft Excel (Version 7.0, Microsoft Corp., Redmond, WA) was used to compute the regression coefficients.

V. RESULTS

Table II summarizes the factorial analyses of variance for the physical parameters of Eq. (3)fo r the "Production" and "Lab" data sets.

The statistical measures of confidence for this analysis are much stronger for the "Production" set, as the "observed *F*" divided by the respective "critical *F*" statistic for each parameter exceeds that of the "Lab" set, usually, by large multipliers. (The observed *F* statistic is a measure of confidence in the sample standard deviations, and is compared to a critical *F* statistic taken from a statistical table for a 95% level of confidence.) The "Production" set has less than 3% coefficient of variation (standard deviation/average) in the four individual parameter cells (in the 2×2 factorial response input matrix) and additionally had more (52, not 12, in Table I), resistor images tested to provide more statistical degrees of freedom with which to lower the standard error.

The "average" parameter values compared between the sets are remarkably similar (3.1%, 4.6%, and −7.4%), with both average *E* values between 1.3 and 1.4 meV. Not so with the "effects" column, which represents the change in a parameter in going from a low level (such as 845 °C) to the respective high level (such as 855 °C), given that 1/2's are used in the contrast matrix. For example, the electrostatic charging energy parameter, *E*, was estimated with higher than 95% confidence only in the "Production" set, wherein the 0.988 correlation value for the R_{b0} parameter is indicative of an excellent analysis in that set. [The correlation coefficient (R^2) is a measure of fraction of raw variability accounted for by the analysis.] The signs of the factors are consistent for both data sets, except for a small negative interaction value for the "Lab" *E*. (The dimension of the interaction column *A*B* is the product of the component units.)

Also contributing is the difference in spans of temperature across the two sets, as listed in part of Table I. Indeed, one should expect a larger effect (in Table II)fo r the 50 °C difference in the "Lab" set than for the 10 °C span in the "Production" set, as determined here. To compensate for the different spans proportionally, the normalized values of Table II were calculated. The ranking orders are the same for the "Temp" and "Time" columns, but large differences remain between the sets. In view of the *F* ratios, conclusions about the process effects are drawn only from the "Production" set.

VI. DISCUSSION

The underlying goal for this study is to relate processing changes (of time and temperature) to changes in the model parameters for the electrical properties. Along the way, we obtained parameter values (for the averages over the tested conditions) with considerable precision, due to the large number of samples used in the parameter estimation for the two-phase resistance model of Pike and Seager.[2] We now link the statistically significant changes in these model parameters to changes in microstructure, which, in turn, are due to changes in the processing factor levels. Although reactions with the electrical terminations and with the substrate additives can also affect the resistance,[4] such effects are minimized by the specimen design and printing method used here.

The parameter value change with the most readily explained physical relationship to processing/microstructure

factors is the electrostatic charging activation energy, E. Through the model, the changes in this value can be directly understood in terms of the coarsening directly observed in the microstructure of the conductive particles in these TFRs.

The resistors are comprised of metallically conductive particles arrayed in a three-dimensional network throughout an insulative matrix. As reasoned earlier for Eq. (1), small, metallically conducting particles embedded in an insulating medium would not have completely degenerate energy levels. In the absence of an applied field, thermal activation with energies on the order of 1 meV result in an equilibrium number of charged particles. With an applied field, electrons tunnel from particle to particle on interconnected chains of particles (or dispersed ones). Larger particles result in more closely spaced energy levels, so the activation energies decrease. Then, with a lower activation energy, there are more thermally charged particles available for conduction.

We directly observed the microstructure coarsening with increasing time and temperature in an earlier paper[9] that qualitatively interpreted processing effects on resistance. Since larger particles have more closely spaced energy levels, electrostatic charging energy drops with higher processing temperatures and longer time at peak temperature, as seen in Table II. The temperature, time, and interaction spans give rise to changes in the E value by -16%, -12%, and $+0.7\%$ of the average value (1.337 meV) for this parameter. Summing the three spans, and distributing the result equally above and below the average value leads to the result that the charging energy decreased from 1.56 to 1.15 meV, with increasing both firing time and temperature. Equivalently, these values are also the cell averages for the (845 °C, 8 min) and (855 °C, 11 min) data in the "Production" set. Additional support for the physical significance of the E parameter is that the average values (which are not subject to the factorial $F_{obs} > F_{crit}$ comparison) between the two data sets (in Table II) compare within 5% of each other: "Production" at 1337 μeV vs "Lab" at 1398 μeV.

The preexponential parameter R_{b0} is taken as a measure of the nontemperature-dependent tunneling resistance of the glass barrier. When the conductive particles coarsen during processing, the barrier layers between particles are expected to thicken. This thickening is independent of whether one is assuming a spatially uniform dispersion of particles or one is assuming a connected topology of chains of particles (as some are seen in Fig. 2), which are individually coarsening with fixed total particle volume. Tunneling is exponentially dependent on barrier thickness and thereby an increased thickness leads to a higher R_{b0}. Thickening of the barrier layer is supported by the present data sets (Table II), which show that R_{b0} increases with both firing time and peak firing temperature factors. It is possible that the R_{b0} parameter may also be affected by the chemical composition within the barrier and/or subtle changes in wetting (also affected by the same process factors) due to changes near interfaces. Recently, Chiang *et al.*[17] have investigated a specialized HRTEM approach to directly observe such compositions in 1–2 nm glass layers.

The smallest effects in proportion to the parameter averages are found for the parameter R_{m0}, the metallic resistance extrapolated linearly to absolute zero. Nevertheless, a good match between the two data sets is found here: The averages for the R_{m0}pa rameter differ by only 7% and the signs of the temperature, time, and interaction effects are consistent. Of any of the tabulated effects on R_{m0}, the largest (in Table II) for the "Production" data set ["Temp" at 1115 Ω/(sq K)] is <5% of the average R_{m0} value. R_{m0} increases both with processing carried out at increased firing temperature and with time held at peak temperature. If such small changes in R_{m0} are physically significant, they may be linked to the chemistry. Our tests[9] with precision lattice parameter measurements show statistically significant differences (but only just at the 95% level) across the wider spans of the Low–Low High–High diagonal of the "Lab" factorial matrix. We interpret this lattice shift as being due to an exchange of the Cu and Bi in the ruthenate phase with Pb in the glassy matrix.

In these systems, the net result of increasing firing time and temperature is to decrease the curvature of $R(T)$ through a decrease in the electrostatic charging energy parameter. This change in curvature can also be related to a decrease in the difference between the (secant) hot- and cold-TCR values, which has been referred to as a "TCR gap,"[4] and also to the quadratic term of earlier nonmodel-based (T, T^2) curve fitting.[3] In processing studies for reaching the lowest magnitude of TCR, we find the electrostatic charging energy, computed from $(1/T, T)$ fitting of the individual $R(T)$ curves, is preferred as a model. Not only does this fitting provide the best fit of data as shown in Fig. 1, it is based on a physicochemical model.

A key benefit in the model-based interpretation is found in using a physical model to seek minimum TCRs. By differentiating Eq. (3) and using values from Table II, the minimum TCR can be found to be slightly below room temperature (as seen in Fig. 1), notwithstanding the antecedent approximations. The lowest TCRs which extend across a nearby range of temperatures are found (in the "Production" set)with the (855 °C, 11 min) processing conditions, where particles have coarsened and E is lowest.

The special four-probe resistor design (Fig. 4) simplified this physical interpretation by exclusion of termination influences, which often give rise to dependencies of TCR (and R) on printed geometry. (The expected influence of any Ag from the terminations is to lower the viscosity of the glass matrix during firing, which is expected to be equivalent to high firing temperatures and longer times.) Likewise, the printing method used provided consistency of resistances (<3% std.dev./average) for the "Production" data set factorial cells that helped keep the standard errors small (in Table II). Taken together, the special design and printing are contributors to why we can directly explain the processing dependence of TCR with the modification in Eq. (3) of the Pike and Seager[2] composite model. The model-based approach allows a deeper physical insight into the processing-microstructure relationships of the thick film resistor systems under study. Furthermore, it will provide linking points to future results from advanced electron microscopy techniques, as they are used to further characterize the detailed structures and chemistry near the interfaces in these resistors.

VII. CONCLUSIONS

With the observed coarsening of the conductive ruthenate particles, increasing closeness of energy levels within larger particles is the basis for the decrease in the electrostatic charging energy, E, of the two-phase resistance model. In the present work, E is shown to decrease from 1.56 to 1.15 meV with increasing processing peak firing temperature (from 845 to 855 °C) and time (from 8 to 11 min).

The $(1/T, T)$ fitting of the model in Eq. (3)co rresponds to a much better match of $R(T)$ (in Fig. 1), than (T, T^2) or secant fitting of Eq. (2). By differentiating Eq. (3), the TCR minimum can be found to be near room temperature. The special four-probe resistor design (Fig. 4) aided this physical model fitting by exclusion of termination influences and reduction of sample-to-sample cross-section variability.

The model parameters and sample design are suggested for use in thick film processing studies which may seek even lower temperature coefficients of resistance through insight into the physical mechanisms of conduction and TCR in thick film resistors.

Further research may allow more correlations of the model parameters with the anticipated advances in nanoscale chemical characterization of thick film resistors.

ACKNOWLEDGMENTS

The authors would like to thank John Healy, Russ Haeberle, Bernadette Piano, David Smith, Ron Haberl, Thuong Pham, Randy Hume, and Achyuta Achari (all of Ford Vision) for technical support and advice; Al Walker, Lyle Slack, and Robert Bouchard (DuPont Experimental Station) for discussion and encouragement; and Roger K. Haboush and Andrew Drews (Ford) for suggestions.

[1] R. J. Bouchard, Ceram. Trans. **33**, 391 (1993).
[2] G. E. Pike and C. H. Seager, J. Appl. Phys. **48**, 5152 (1977).
[3] J. Lee and R. W. Vest, IEEE Trans. Compon., Hybrids, Manuf. Technol. **CHMT-6**, 430 (1983).
[4] T. Pfeiffer and R. J. Bouchard, Ceram. Trans. **33**, 405 (1993).
[5] A. T. Walker, L. A. Silverman, K. W. Hang, T. Pfeiffer, V. P. Siuta, L. H. Slack, and R. J. Bouchard, Proc. SPIE **2105**, 695 (1993).
[6] B. Morten, A. Masoero, M. Prudenziati, and T. J. Manfredini, J. Phys. D **27**, 2227 (1994).
[7] G. E. P. Box, W. G. Hunter, and J. S. Hunter, *Statistics for Experimenters* (Wiley, New York, 1978), p. 306.
[8] N. Koppetzki, Cryogenics **23**, 559 (1983); H. Doi, Y. Narahara, Y. Oda, and H. Nagano, in *Proceedings of the 17th International Conference on Low Temperature Physics, LT-17*, edited by U. Eckern, A. Schmid, W. Weber, and H. Wuhl (North-Holland, Amsterdam, 1984), Vol. 1, p. 405.
[9] F. Johnson, G. M. Crosbie, and W. T. Donlon, J. Mater. Sci.: Mater. Electron. **8**, 29 (1997).
[10] R. Stratton, J. Phys. Chem. Solids **23**, 1177 (1962).
[11] B. Abeles, RCA Rev. **36**, 594 (1975).
[12] C. A. Neugebauer and M. B. Webb, J. Appl. Phys. **33**, 74 (1962).
[13] C. H. Seager and G. E. Pike, *Sandia Technical Report SAND76-0536* (NTIS, Washington, DC, 1976).
[14] R. Holm, J. Appl. Phys. **22**, 509 (1959).
[15] J. Frenkel, Phys. Rev. **36**, 1604 (1930).
[16] S. B. Vardeman, *Statistics for Engineering Problem Solving* (PWS, Boston, 1994), p. 582.
[17] Y. M. Chiang, L. A. Silverman, R. H. French, and R. M. Cannon, J. Am. Ceram. Soc. **77**, 1143 (1994).